



## Using GPR Technique Assessment for Study the Sub-Grade of Asphalt and Concrete Conditions

Alaa S. Mahdi

Remote Sensing Unit, College of Science, University of Baghdad, Baghdad, Iraq

### Abstract

The Ground Penetrating Radar (GPR) is frequently used in pavement engineering for road pavement inspection. The main objective of this work is to validate nondestructive, quick and powerful measurements using GPR for assessment of sub-grade and asphalt /concrete conditions. In the present study, two different antennas (250, 500 MHz) were used. The case studies are presented was carried in University of Baghdad over about 100m of paved road. After data acquisition and radar grams collection, they have been processed using RadExplorer V1.4 software implementing different filters with the most effective ones (time zero adjustment and DC removal) in addition to other interpretation tool parameters.

The interpretation results showed that with 250 MHz antenna, the buried plastic pipe and the flexible pavement layer were identified. The later appeared as one layer without identifying the rigid pavement layer. With 500 MHz antenna, the plastic pipe, rigid pavement, appeared clearly. Moreover, the short type of maximum time window using antenna 500 MHz appeared to be the most suitable for detecting some radar anomalies (plastic pipe, and pavement thickness) which were clearly defined. While, the suitable radar wave velocity was 100 m/ns for estimation of the flexible and rigid pavement layer thicknesses respectively. No change is obtained with changing point interval. . Finally, this diagnostic tool of GPR for pavement defects and damages investigations seems very promising, cost effective and efficient in its implementation.

### استخدام تقنية رادار اختراق الأعماق لدراسة الطبقات الإسفلتية والكونكريتية

علاء سعود مهدي

وحدة الاستشعار عن بعد، كلية العلوم، جامعة بغداد، بغداد، العراق

### الخلاصة

يعتبر رادار الاختراق الأرضي من التقنيات الحديثة المستخدمة في هندسة الطرق والترصيف. الهدف من الدراسة فحص وتصديق طبقات الطرق المعيدة ضمن المواصفات الهندسية. استخدم لهذا الغرض هوائيات للرادار ضمن الترددات (250، 500 MHz). تقع منطقة الدراسة ضمن مجمع جامعة بغداد وطول الطريق المعبد حوالي 100 متر. تم جمع البيانات واستخلاصها من ذاكرة الجهاز ثم عولجت بالبرنامج الجاهز الخاص بالرادار (RadExplorer V1.4) مع استخدام مرشحات متعددة لغرض تحسين الإشارة ودقة القراءات، لقد تبين من خلال الدراسة بان أفضل المرشحات هي: Time zero adjustment and DC removal.

لقد أظهرت نتائج التفسير للبيانات بان استخدام الهوائي 250 MHz قد بين منطقة الدراسة على شكل طبقة واحدة بدون تحديد مكوناتها من الطبقات (مكون واحد)، كما اظهر استخدام هذا الهوائي وجود أنبوب بلاستيك داخل الطبقة. في حين أظهرت قراءات الهوائي 500 MHz طبقات متعددة للطريق مع سمك كل طبقة ووضوح أكثر بالإضافة إلى كشف الأنبوب أنف الذكر. لقد تبين من خلال البحث وجود علاقة وثيقة بين دقة القراءات ومعايرة متغيرات الهوائي سرعة الموجة في الوسط 100 m/ns. أخيراً نلاحظ أن استخدام هذه التقنية تقلل من الوقت، الجهد، والكلفة.

## Introduction

Ground penetrating radar (commonly called GPR) is a high resolution electromagnetic technique that is designed primary to investigate the shallow subsurface of the earth, building materials, roads and bridges. GPR is a relatively new geophysical tool that has become increasingly popular due to its high resolution and the need to better understand near-surface conditions. GPR methods use electromagnetic energy at high frequencies (10 to 4000 MHz) to probe the subsurface, and the propagation of the radar signal depends on the electrical properties of the ground at the high frequency, [1]. The GPR methods measure the velocity and attenuation of the radar waves, and these can be used to determine the dielectric constant or relative permittivity, which is the major electrical property of geological materials at high frequencies. GPR as a non-destructive method uses electromagnetic radiation in the microwave band (UHF/VHF Frequencies) of the radio spectrum, and detects the reflected signals from subsurface structures. The impulse of Ground Penetrating Radar (geo radar) is a precise transmitting-receiving measuring device, which implements the phenomenon of reflection of electromagnetic waves. The transmitting antenna sends an interrupted sinusoidal impulse of the length of one and a half period. The electromagnetic waves travel with radar velocity, which is dependent on electromagnetic properties of penetrated material. The delay results from the distance between the transmitting antenna, underground reflectors (any material with different electrical properties to source materials, which reflects a part of the energy of electromagnetic, [2, 3].

## Theory of the GPR

The ground penetrating radar method is based upon the transmission of pulsed electromagnetic waves. In this method, the travel times of the waves reflected from subsurface interfaces are recorded as they arrive at the surface, and the depth,  $D$ , to an interface is given by, [4, 5];

$$D = \frac{TV}{2} \quad (1)$$

Where:

$D$  is the depth to the reflector.

$V$  is the velocity of the radar wave pulse through the subsurface material.

$T$  is the two-way travel time to the reflector (taken from the GPR trace).

The conductivity of the ground imposes the greatest limitation on the use of radar probing, that is, the depth to which radar energy can penetrate depends upon the effective conductivity of the strata being probed. This, in turn, is governed mainly by the water content and its salinity. Furthermore, the value of effective conductivity is also a function of temperature and density, as well as the frequency of the electromagnetic waves being propagated. The least penetration occurs in saturated clayey materials or where the moisture content is saline. For example, attenuation of electromagnetic energy in wet clay and silt means that depth of penetration frequently is less than 1 m. The technique appears to be reasonably successful in sandy soils and rocks in which the moisture content is non-saline. Rocks such as limestone and granite can be penetrated for distances of tens of meters and in dry conditions the penetration may reach 100 m. Ground probing radars have been used for a variety of purposes in geotechnical engineering, for example, the detection of fractures and faults in rock masses, the location of subsurface voids and the delineation of contaminated plumes [1, 3].

GPR uses transmitting and receiving antennas or only one containing both functions. The transmitting antenna radiates short pulses of the high-frequency (usually polarized) radio waves into the ground. When the wave hits a buried object or a boundary with different dielectric constants, the receiving antenna records variations in the reflected return signal. The principles involved are similar to reflection seismology, except that electromagnetic energy is used instead of acoustic energy, and reflections appear at boundaries with different dielectric constants instead of acoustic impedances [6].

It is known that most of soils and rocks have very low conductivity (about  $< 10^{-2}$  S/m) thus the electromagnetic waves propagation is mainly affected by electrical dielectric constants of soils and rocks. The applied frequencies used are considered low compared with that of Radar frequencies to ascertain their penetration inside earth layers.

The propagation of the radar signals into earth layers depends upon the electromagnetic properties of soils and rocks which are dielectric Permittivity  $\epsilon$  and electrical conductivity ( $\sigma$ ).

Thus, if these properties are changed abruptly at the layer interfaces so part of the energy will be reflected as in seismic reflection. The propagation of electromagnetic (EM) waves at frequencies in the range of megahertz (radar pulse) is mainly controlled by the dielectric properties of the rock material. The radar pulse is reflected from a boundary, so that  $V=(2D)/T$ . The velocities of propagation of radar signal are related to the relative dielectric constant relative permittivity (or relative dielectric constant)

( $\epsilon_r$ ):

$$V = \frac{c}{(\mu_r \epsilon_r)^{1/2}} \quad (2)$$

Where  $\epsilon_r (= \epsilon/\epsilon_0)$  is the ratio of the dielectric permittivity of the medium to the dielectric permittivity of free space ( $=8.85 \times 10^{-12}$  F/m),  $\mu_r (= \mu/\mu_0)$  is the relative permeability of the medium which is about unity for most earth soils and rocks, and  $c = 3 \times 10^8$  m/s ( $=0.3$  m/ns) is the velocity of EM waves in free space. Since  $\mu_r$  is close to unity for most rock materials (accept a few strongly magnetic rocks), radar velocity is primarily controlled by the dielectric constant of the medium as  $\mu_r \approx 1$ :

$$V = \frac{c}{(\epsilon_r)^{1/2}} \quad (3)$$

Table 1 lists typical values of radar parameters for some common materials. Velocities are generally well below the 0.30 m/ns (300 000 km/s) velocity of light in free space. In comparison with water for which  $\epsilon_r = 81$ , most geological formations have much lower values, the lowest values (in the range 3–10) being dry sand/gravel and silt, unaltered hard rocks, permafrost soils and ice. The relative dielectric constant ( $\epsilon_r$ ) varies from 1 in air to 81 in water. For most geologic material,  $\epsilon_r$  lies in the range 3 – 30. Consequently, the range of radio wave velocities is large from around 0.06 to 0.175 m/ns as shown in Figure 1.

Water plays an important role in the attenuation of the EM waves and it affects the GPR survey. The higher conductivity of the materials subjected to survey the higher the attenuation of the electromagnetic waves penetrating the media and therefore the less we can "see" into the ground. Electrical conductive media are salt water, and some types of clay particularly if they are wet. Agricultural soils containing soluble fertilizer like nitrogen or

potassium can be highly conductive as well. How does water affect the GPR survey? Soils-containing water has high electrical conductivity. Water particles absorb energy with high frequency ( $> 1000$  MHz).

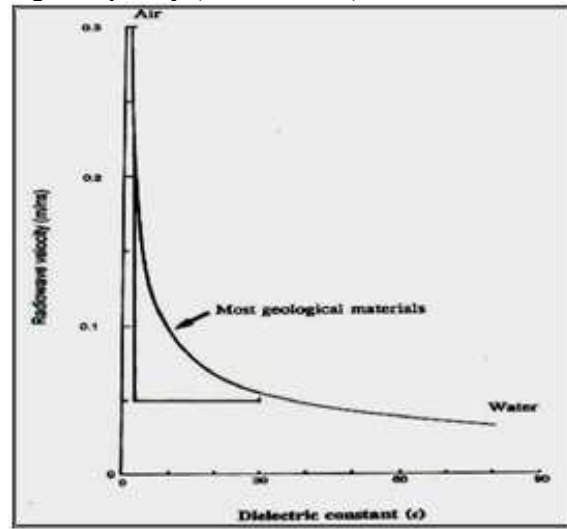


Figure 1- The varying of dielectric constant as a function of radio wave velocity, [7].

Thus, high frequencies are used for shallow depth investigations, while low frequencies are used for large depth investigations. The depth range of GPR is limited by the electrical conductivity of the ground, the transmitted center frequency and the radiated power. As conductivity increases, the penetration depth also decreases. This is because the electromagnetic energy is more quickly dissipated into heat, causing a loss in signal strength at depth. Higher frequencies do not penetrate as far as lower frequencies, but give better resolution. Optimal depth penetration is achieved in ice where the depth of penetration can achieve several hundred meters. Good penetration is also achieved in dry sandy soils or massive dry materials such as granite, limestone, and concrete where the depth of penetration could be up to 15 m. In moist and/or clay laden soils, saturated concrete and soils with high electrical conductivity, penetration is sometimes only a few centimeters. The depth of penetration is related with the electrical conductivity by the following general formula:

$$D=35/\sigma \quad (4)$$

Where  $D$  is the depth of penetration in m and  $\sigma$  is the electrical conductivity in (ms/m), [8].

**Table 1-** Typical values of radar parameters for some common materials, [9]

Material	$\epsilon$	$\sigma$ mS/m	V m/ns	$\alpha$ dB/m
Air	1	0	0.30	0
Ice	3–4	0.01	0.16	0.01
Fresh water	80	0.05	0.033	0.1
Salt water	80	3000	0.01	1000
Dry sand	3–5	0.01	0.15	0.01
Wet sand	20–30	0.01–1	0.06	0.03–0.3
Shales and clays	5–20	1–1000	0.08	1–100
Silts	5–30	1–100	0.07	1–100
Limestone	4–8	0.5–2.0	0.12	0.4–1
Granite	4–6	0.01–1	0.13	0.01–1
(Dry) salt	5–6	0.01–1	0.13	0.01–1

### Applications of GPR in Road Assessment

GPR has been used successfully in a variety of highway applications including: 1) Measuring layer thickness of asphalt pavements, concrete pavements, and granular base layers; 2) Estimating asphalt densities; 3) Determining moisture content of base materials; 4) Identifying stripping zones in asphalt layers; 5) Detecting air-filled and water-filled voids; 6) locating subsurface vertical cracks; 7) Locating subsurface “anomalies” including buried objects, peat deposits, and near-surface bedrock; and analyzing rutting mechanisms, [10].

### The objectives of the Study

The aim of this study was included.

1. Utilizing ground penetrating radar with different frequencies (250, 500 MHz) and studying the properties and performance of this technique for pavement engineering.
2. Testing the different operating setting parameters and their effects in accuracy and interpretation of GPR radar grams.
3. Extracting the geometric characteristics of road paved surfaces, in order to evaluate the conditions of sub-grade and asphalt/concrete and detecting any subsurface damages with diagnosis.

### Pavements

Pavements are planar-layered media with different materials composing each layer. Based on their main components, pavements are divided into three categories, [11]: Flexible (Hot-Mix Asphalt) pavements (HMA), rigid (concrete) pavements (CP), and composite pavements (AC).

#### • Flexible Pavements

Flexible pavements are layered systems composed of different layers that are placed in such a way that layer strength is greater at the top, where the stresses caused by traffic loading are high. This approach allows cheaper local materials to be used in pavement construction. As depicted in figure (4), flexible pavements can be composed of the following, [12]:

- **Surface course** (or **wearing surface**) is the top layer of a flexible pavement. It is constructed by a dense graded hot-mix asphalt (HMA) material. This mix provides a balance in aggregate size, where a high resistance to traffic-load requires large aggregate and a smooth and skid-resistant riding surface requires strong, small aggregate. The wearing surface thickness is usually between 25mm and 50mm.

- **Binder course** (or **asphalt base course**) is an HMA layer that is composed of larger aggregates and less asphalt binder content than the surface course. Because of its low asphalt binder content, the base course resistance to fatigue cracking is less than the surface mix. The lower resistance to cracking is justified by the lower stresses applied to the base course layer since it is deeper in the pavement. To ensure bonding between the two HMA layers, tack coat (asphalt emulsion) is usually sprayed over the bottom layer before placing the top layer. The asphalt base course thickness usually varies between 50mm and 250mm, figure 2.

- **Base course** is a layer composed of crushed stone that can be either untreated (loose) or stabilized (by adding small quantities of cement or asphalt). The base course is usually 100mm to 300mm thick.

- **Sub-Base course** is similar to the base course; however, it is typically composed of lower quality (weaker) aggregates for economic reasons. The sub-base course is usually 100mm to 300mm thick.

- **Sub-grade** is the bottom layer supporting all the aforementioned layers. It can be either the original in-situ soil or a placed layer of selected material. In both cases, the sub grade should have a high density attained by good compaction.



Figure 2- Flexible pavement road section

It should be noted that a typical pavement is composed of any combination of two or more layers in the order specified above (top to bottom). A flexible pavement should have, at least, an HMA layer and an aggregate (base course) layer. The layer thicknesses used in the design depend primarily on the importance of the road, the volume of traffic it is expected to carry, the properties of the construction materials used, and the local environmental conditions. Some flexible pavements, known as full-depth asphalt pavements, have a unique 50mm to 100mm (2in to 4in) wearing surface layer and a 50mm to 510 mm (2in to 20in) asphalt base course, [11].

Flexible pavement distresses are mainly due to repeated traffic loading and to varying environmental conditions, such as temperature, rain, and frost. Distresses could appear directly on the surface of the pavement (wearing

surface) in the form of cracks or potholes, in which case they are visible and, therefore, are easily detectable by visual inspection. Distresses could also start underneath the surface, propagating over time until they reach the surface. These internal defects are typically caused by extensive loading, weak sub grade, and/or entrapped moisture. Moisture accumulates in the sub grade or the aggregate base layers, causing a decrease in the material resistance to permanent deformation caused by heavy traffic loads. Moisture can also be trapped within the HMA layers, thus producing rupture in the bond between asphalt and aggregates, which can result in raveling (disintegration of the surface), bleeding (asphalt binder movement to the surface), and a weak layer [11].

#### Rigid Pavements

Rigid pavements are constructed of 150mm to 300mm Portland cement concrete (PCC) slabs. The slabs can be placed either directly on the prepared sub grade surface or on a 100mm to 300mm thick granular base layer. Four types of PCC pavements can be identified based on the reinforcement configuration [5].

Rigid pavement distresses are essentially due to repeated traffic loading and to varying environmental conditions. These distresses may be divided into two categories: distresses caused by the base (or sub grade) layer failure and distresses originating in the concrete slab itself. The first category is caused by weakening of the base (or sub grade) layer either due to moisture accumulation or material loss produced by soil and particle pumping at the slab joints or the existing cracks. The second category can be due to the corrosion of the steel rebar in reinforced concrete, joint faulting, freezing and thawing, alkali-silica reaction in concrete, and/or other chemical attacks.

#### Composite Pavements

Composite pavements are composed of concrete slabs overlaid by HMA, thus providing the simultaneous strength of concrete as a base layer and the smoothness of HMA. Due to the high cost of such pavements, they are rarely constructed as new pavements; however, they usually result from the rehabilitation of old concrete pavements by adding an HMA overlay at an appropriate thickness. Flexible pavements may also be overlaid with concrete, which is known as white topping, [10, 13].

Distresses in composite pavements are similar to those found in flexible pavements. However, a characteristic crack type, the joint reflection cracking, is usually found in HMA layers overlaying jointed concrete slabs. This type of cracking starts at the concrete joints and propagates over time towards the surface.

#### **The Field Work**

The fieldwork was performed within a 13 days starting from 13/3/2013 to 25/3/2013, and included the using of MALA GPR (Sweden) survey using different utility functions (available antennas, survey speed, sampling frequency, maximum time window, velocity ,etc.) to choose the best function both in accuracy and in interpretation. The study was performed in the University of Baghdad over about 100m of paved road.

The antenna frequencies of GPR used in this study was two types namely 250 MHz, 500 MHz.

The filters used in this study are:

Time zero adjustment, DC Removal, Background removal, Amplitude correction, Automatically gain control (AGC), Spherical divergence correction, Trace equalization, Band passes flitter, Stoat-*K* migration.

#### **The Geology of Study Area**

Baghdad is located in the middle part of Mesopotamian Plain. Baghdad soil site strata are fluvial affected by river causing changes during previous decades leading to different depositional stratigraphy each few meters, thus Baghdad strata are erratic, somewhat are homogenous with water table near the ground, [9].

#### **The Data Editing**

Data editing is the first processing procedure which was applied on the collected profiles (raw data). The editing includes reorganization

and renaming the recorded files. For example DAT\_08\_A1 to profile which was achieved for the selected straight line in the University of Baghdad and registering the operation setting parameters of GPR such as: the center frequency 250, 500 MHz, time windows 61.9 ns, point interval 0.030 m, sampling frequency 8110.71 and velocity 100 m/ns.

#### **Data Processing**

The collected profiles (raw data) in this study are presented in 2D sections (radar grams). The field profiles (that come without any type of processing) are then imported into RadExplorer V 1.4 software for radar gram processing. The field raw data were conducted by changing the operation setting of GPR (antenna, Max time window, EM wave velocity and point interval). In the following sections, the raw data will be shown with the processed data side by side, [14].

#### **Operation Setting of GPR on Paved Roads**

A specific and straight line was chosen as a tested profile as shown in figure 3. This work was carried out to select the suitable antenna; suitable Max. Time Window, suitable Point Interval, and suitable EM wave velocity.

To choose the most appropriate antenna, two different frequencies (250, 500 MHz) were used which were available in the College of science/ Remote Sensing Research Unit. the operation setting parameters of GPR. These antennas were used respectively on the profile. The raw data radar grams of this test are shown in figure 3. The change in maximum time window (short or medium) was applied for the two antenna frequencies (250, 500). This work was achieved for selected straight line within the site as shown in figure 4-a, Table 2 shows the operation setting parameters of GPR. While figure 4 shows the raw data radar grams for this test.

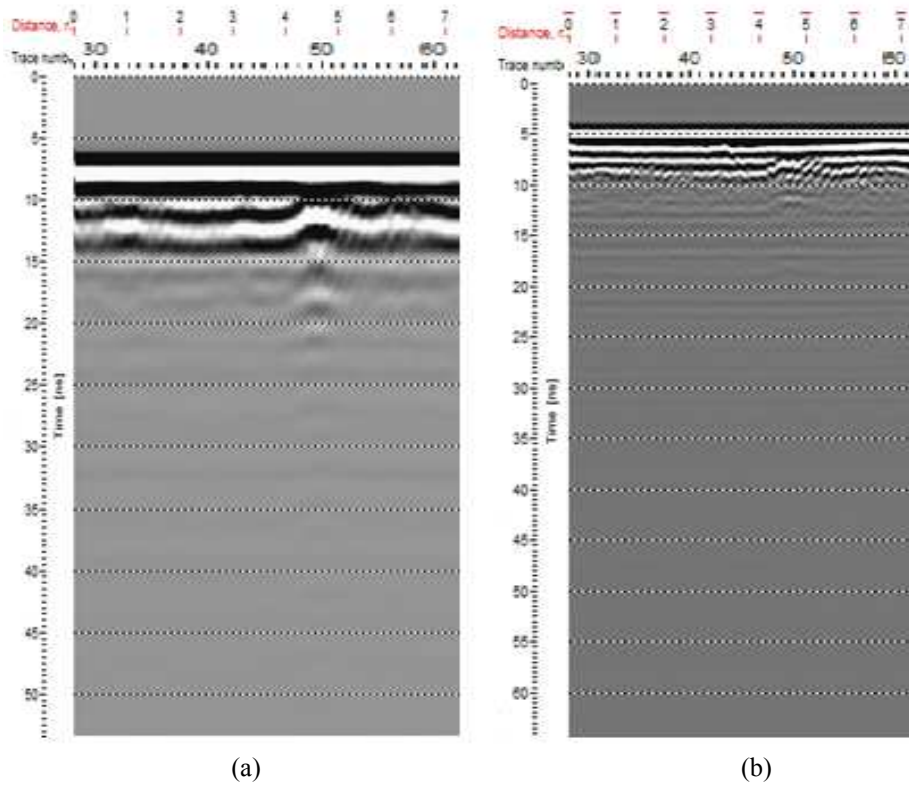


Figure 3- Radargrams for the investigated site using antenna with:(a) 250MHz, (b) 500 MHz

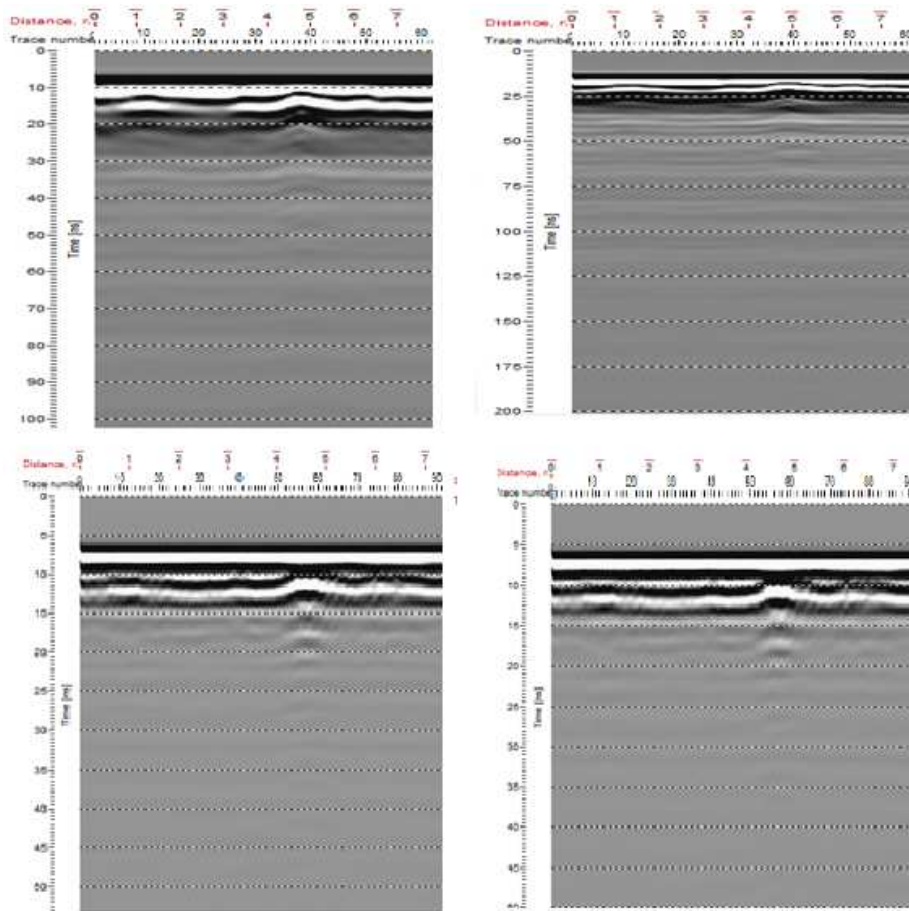


Figure 4- Changing maximum time window for the used antennas:  
(a) 250 MHz, Short, (b) 250MHz, Medium, (c) 500MHz, Short, (d) 500MHz, Medium

The range of used velocity is (10-160) m/ns. Practically, the GPR display shows only the depth value which automatically changes

according to velocity value as shown in table 2, some of raw data radar grams for this test are shown in figure 5.

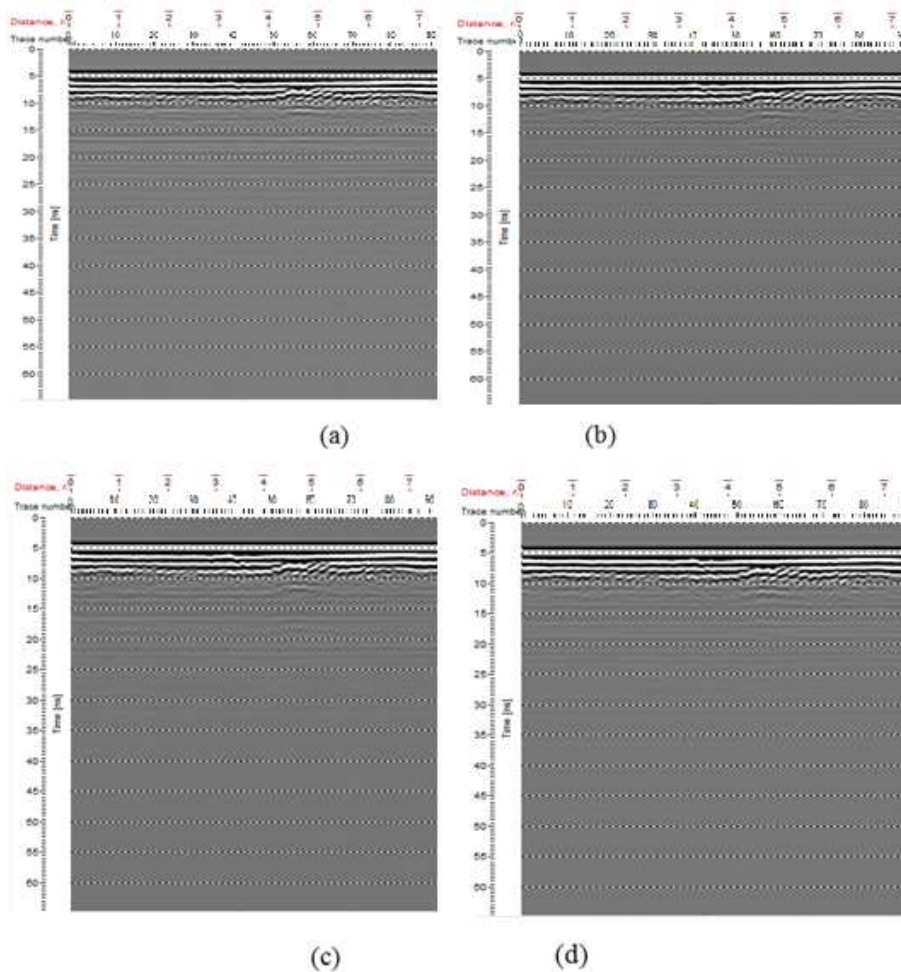


Figure 5 - Changing EM wave velocity (a) 10m/ns, (b) 60 m/ns, (c) 100 m/ns, (d) 160 m/ns.

Point interval is the distance between each trace collected for all individual channels. This test was carried out along the same selected profile as shown in figure 4-a. The parameter screen of

GPR shows that all parameters values are fixed, so no change appeared as shown in table 2, Some of raw data radargrams for this test are shown in figure 6.

Table 2- Operation setting of GPR, changing max. time window.

Parameter Setting	Antenna			
	250 MHz		500 MHz	
Max. Time Window	Short	Medium	Short	Medium
Velocity (m/ns)	100	100	100	100
Time Windows (ns)	191.8	191.8	46.1	46.1
Point Interval (m)	0.05	0.05	0.03	0.03
Sampling Freq. (MHz)	4883.87	2492.4	5064.66	5340.86
Depth (m)	9.77	9.77	2.39	2.39



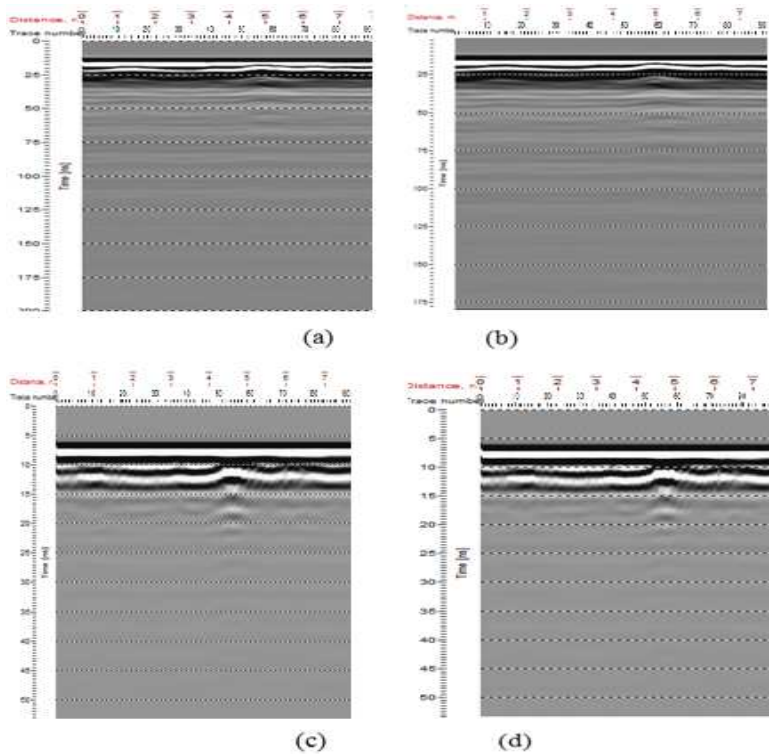


**Figure 6-** Changing point interval for antennas  
 (a) 250 MHz , 0.05m ,(b) 250 MHz, 0.1m,(c) 500 MHz , 0.03m , (d) 500 MHz

**Filters Processing**

Filtering of radar data is used as an attempt to remove the unwanted signals (noise), and correcting the position of reflectors on the radar record. The steps of applying the filters depend upon the accuracy of collected profiles and the aim of survey. Each case of the profiles has different processing procedure. All the profiles in this study were processed with the same range of the filters values, because the studied area contains pavement layer, which have approximately same original characteristics. There are several types of filters on the right side of the RadExplorer software screen figure7.

The list of the filters mentioned in figure below includes the main effective filters implemented for the profiles of the studied area in addition to non-effective filters. Not all filters have been used, some of the non-effective filters are mentioned as samples to show their influence or deformation. While, the other ones are effective. The most common filters which have been used are DC Removal and Time-Zero Adjustment. In the same time, the other filters show deformity for the radar grams and being not useful for the study objectives.

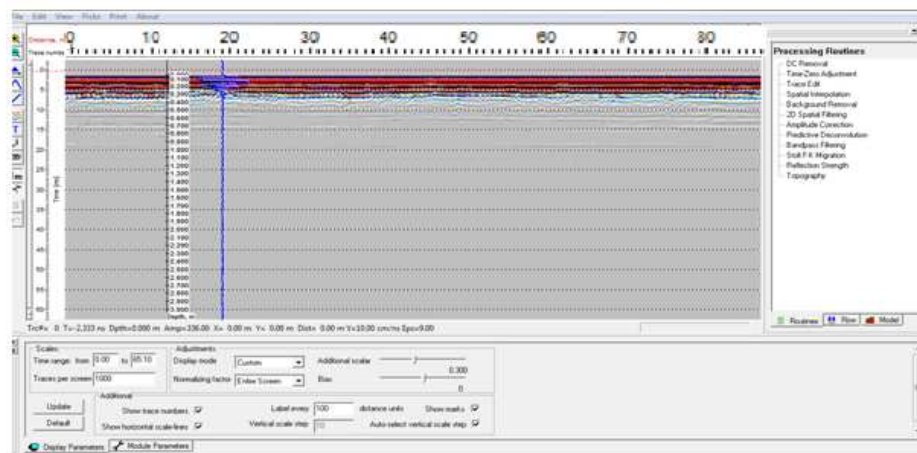


**Figure 7-** The raw data (radar gram) inside the processing software

**Time Zero Adjustment Filter**

The “Time Adjustment” filter is used for adjusting the zero-point of the vertical time scale to the time-zero, the moment when the wave has actually left the emitting antenna. Applying this filter can set the direct wave arrival time. At the

same time in the visualization window, the white horizontal dotted line that defines the first-arrival time position is moving [15, 16]. The adjustment of this filter can be shown in Figures 8 and 9. This filter was applied for all the profiles.

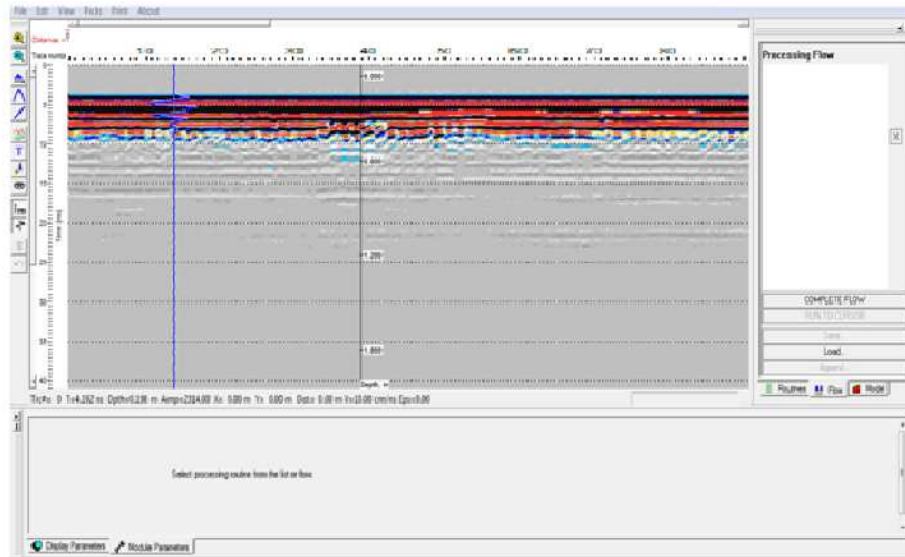


Figure 8-Profile No.248 Before Applying The Time Adjustment Filter

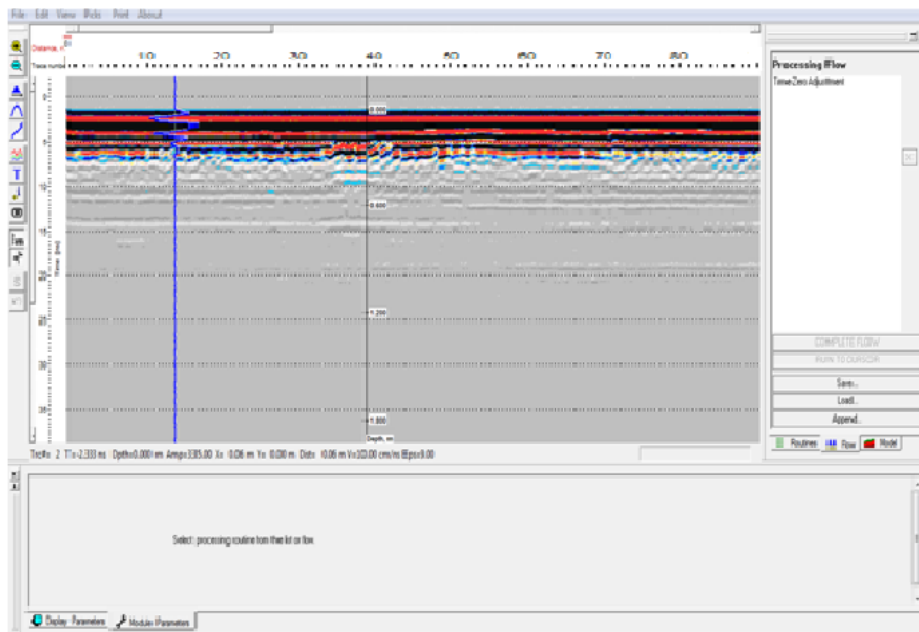


Figure 9- Profile No.248 After applying the time adjustment filter with first arrival time 2.8 ns

**The DC Removal Filter**

The “DC Removal” filter is used to remove constant component (DC component) of the signal in case there is one [7]. The implementation of this filter is shown in figure

10. This filter was applied for all profiles as this filter processing gives an enhancing step of the resolution so it is considered as an effective filter.

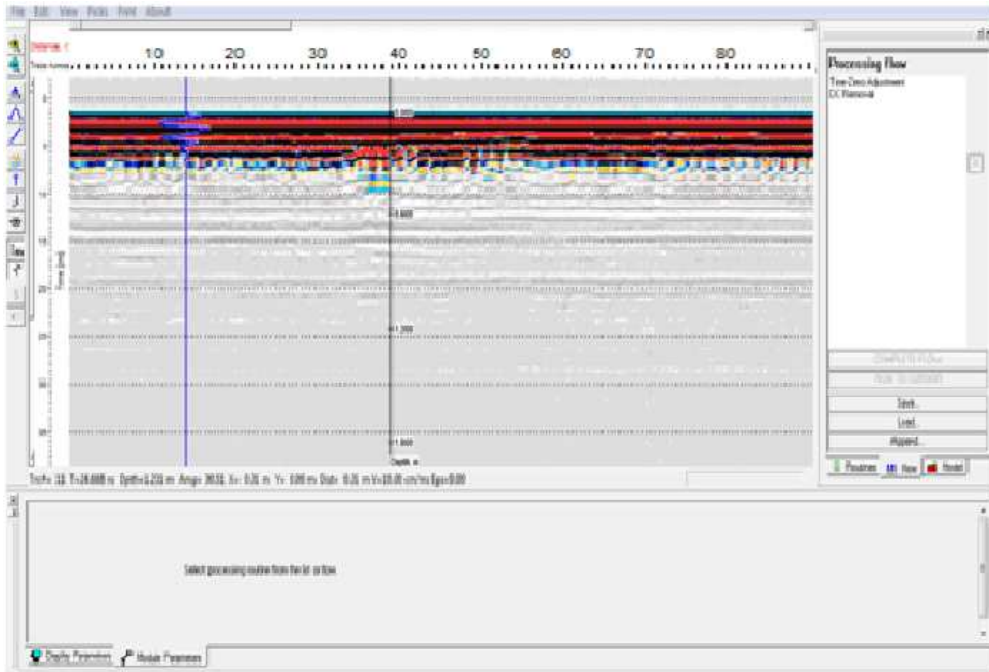




Figure 10- Profile No.248 after applying the dc removal filter

**Interpretation of the Tested Profiles**

**First Step:** For all profiles, applying “Floating depth ruler” button and “Trace” button.

**Floating depth ruler:** It is a  depth scale that shows the depth expressed in meters (or feet) in accordance with the current velocity model.

**Trace:**  this buttons used to display a single wiggle trace above the radargram.

**Second Step:** Applying “Pick” by pressing the button picking mode on/off, then changing the parameter setting of pick in tool bar to AUTO FILL in (Peak, neg2pos and pos2neg) mode. After activation “Horizontal Pick”, lining the top and bottom of layers in radargram can be identified and assigned as shown in figure 11

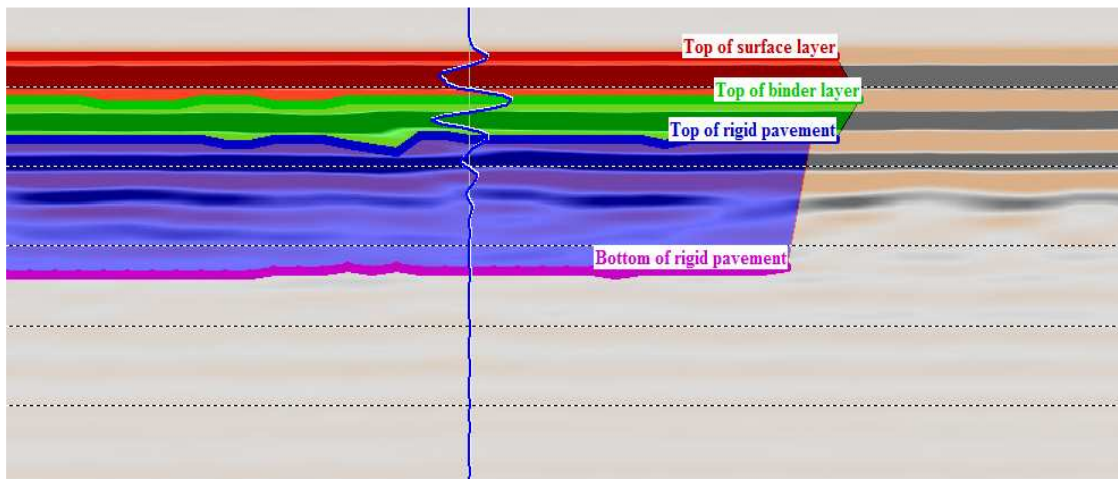


Figure 11- Identifying the boundary of layers using pick and fill the layer using the model option

**Third Step:** Exporting the “Horizontal Pick” as a text file, [17, 18].

1. The first line contains the name of the pick.
2. The second line describes the table columns. The column names are separated by columns. Which contains X and Y coordinates, trace

number, two-way time, and depth calculated from the time according to current velocity model.

3. Then there is an empty line that is followed by the number of points (nodes) in the pick.

4. The following line contains some service information: line type code, line width, colour code.

5. Then the space-delimited values follow. Each node of the pick corresponds to a row in the table. The order of the values in a row corresponds to what is described in the second line of the file.

**Fourth Step:** Importing the “Horizontal Pick” text file to Excel Work sheet to make the calculations for layer pavement thickness.

Selecting suitable antenna is important in accuracy and interpretation to the pavement layer thickness. Two antenna frequencies (250, 500, MHz) were used. The operation setting presented in figure 12 shows the radar gram of profile No. 264 for antenna center frequency 250 MHz in which the plastic pipe appeared

with dielectric constant equal to 2.9 with velocity equal to 17.7 cm/ns at depth 0.377 m from the surface. And as shown the pavement layer thickness did not clearly appear by using antenna 250 MHz.

But by using antenna 500 MHz for profile No.260, the plastic pipe was appeared clearly with this antenna than with antenna 250MHz. Besides in the rigid pavement, the steel reinforcement bars and sheet cork that was used in joint were appeared. For cork sheet, the dielectric constant equals to 15.8 with velocity equal to 7.5 cm/ns at depth 0.25m from the surface. While for the steel reinforcement bar, the dielectric constant equals to 13.6 with velocity equal to 8.1 cm/ns as shown in figure13.

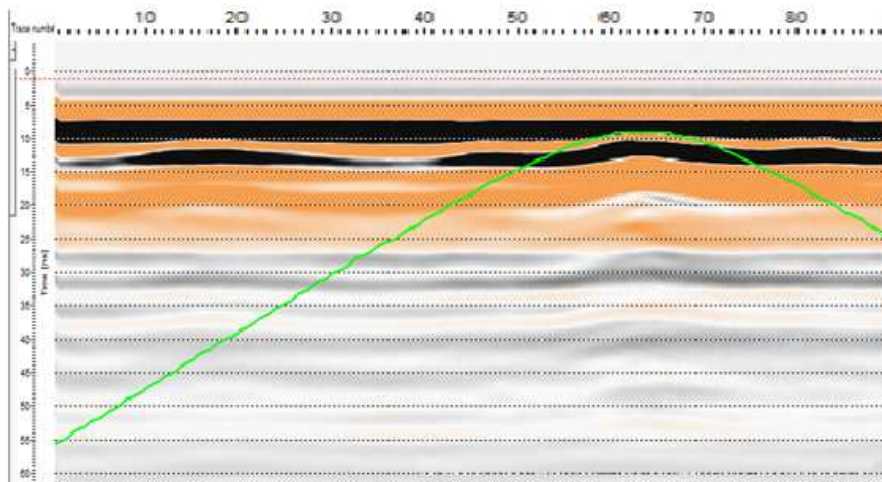


Figure 12- Using antenna 250 MHz on profile No.264 where Plastic Pipe was appeared.

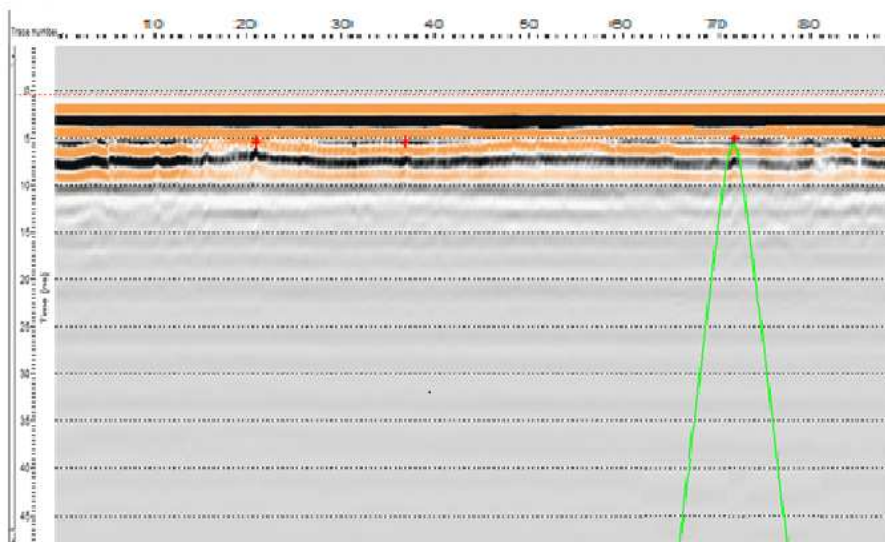


Figure 13- Using antenna 500 MHz on profile No.260 where cork sheet was appeared

**Conclusions**

In this study, the GPR was implemented as a nondestructive, quick low cost and powerful technique for assessment of asphalt/concrete conditions. This study has been chosen for two different antennas (250, 500 MHz). The case studies presented were carried out in the University of Baghdad over about 100m of paved road. The main conclusions can be summarized as follows:

1. In general, after data acquisition and processing using RadExplorer V1.4 software and implementing different filters, it was found that the most effective ones are time zero adjustment and DC removal in addition to other interpretation tool parameters.

2. This diagnostic tool of GPR for pavement defects and damages investigations seems very promising, cost effective and efficient in its implementation.

3. The surveys have shown the potential for overcoming some of the inherent limitations of GPR (i.e., the need for careful antenna frequency selection and survey design in order to image through complex rebar meshes) and can produce results that are equally accurate from an interpretational point of view.

4. The interpretation results of this case showed that, working with 250 MHz antenna, the buried plastic pipe and the flexible pavement layer are identified. The flexible pavement layer appeared as one layer while the rigid pavement layer is unresolved.

5. With 500 MHz antenna, the plastic pipe, rigid pavement, steel reinforcement bars and joint sheet cork appeared clearly.

6. While, no change is noticed on radargrams when applying different point intervals.

7. The suitable radar wave velocity for estimating the thicknesses of the surface, binder and rigid pavement layers were 10,160 m/ns respectively.

## References

1. Annan A. P., and COSWAY S. W, **1992**, "Simplified GPR beam model for survey design", Society of Exploration Geophysicists, New Orleans, USA.
2. Baradello, L, Acquisition and Processing of GPR Data. <http://web.interpuntoen.it/baradello/georadar-processing>.
3. Chen, J., **2001**, "Bayesian Approaches for subsurface characterization using Hydro geological and Geophysical Data". Ph.D. Thesis Engineering. Civil and Environmental Engineering. University of California, Berkeley.
4. Daniels, J.J., **2000**, "Ground Penetrating Radar Fundamentals", published report, Department of Geological sciences, Ohio State University, Region V, pp:1-21.
5. Environmental Protection Agency. Ground Penetrating Radar. ([http://www.epa.gov/region5superfound/sfd\\_fss/htm/gpr.htm](http://www.epa.gov/region5superfound/sfd_fss/htm/gpr.htm)).
6. Davis, J.L, Annan, A.P., **1989**, "Ground penetrating radar for high- resolution mapping of soil and rock stratigraphy". *Geophysical prospecting*. Vol. 37, pp. 531-551.
7. Natural Resources Conservation Services (NRCS), **2008**, Methodology of ground penetrating radar. <http://GPR.NRCSsoils>.
8. Department of Transportation (DOT), **2006**, "Feasibility of using ground penetrating radar (GPR) for pavements, utilities, and bridges". Federal Lands Highway program; Borehole logging. <http://www.cflhdgov/agm/index.htm>.
9. N.C.C.L. (National Center for Construction Labs), **1986**, "A Study of the Engineering Soil Characteristics of Baghdad Area", Al-zaman publication house Baghdad.
10. Liken, M. C., **2007**, "Use of Ground Penetrating Radar to Evaluate Minnesota Roads", Minnesota Department of Transportation, pp:4-10.
11. Lamoure, S., **2003**, "Development of Data Analysis Algorithms for Interpretation of Ground Penetrating Radar Data", Ph.D. in Electrical engineering submitted to the Faculty of the Virginia Polytechnic Institute and State University.
12. Huang, Y.H., **2004**, "Pavement Analysis and Design". Second addition, New Jersey: Prentice Hall.
13. Maerz, N. H, Kim, W., **2000**, "Potential Use of Ground Penetrating Radar in highway Rock Cut Stability", a Research Published in Internet, <http://web.mst.edu/~norbert/pdf/gpr.pdf>, 9 P.
14. RAMAC/GPR, **2005**, "Antennas, Operating manual", Version 1.1, [www.malags.com](http://www.malags.com).
15. MALÅ Operating manual, **2005**, "MALÅ XV Monitor with Professional Firmware", Version 1.5, from <http://www.malags.com>.
16. Milsom, J., **2003**, "Filed Geophysics", third addition, University College London.
17. Park, Y. J., Kim, K. H., Cho, S. B., Yoo, D. W., Youn, D. G., Jeong, Y. K., **2004**, "Development of a UWB GPR System for

Detecting Small Objects Buried under Ground”, a Research published in internet, 3 Pages.Iraq Virtual Science Library <http://www.ivsl.org>.

18. RadExplorer 1.4, **2005**, “The software for GPR data processing and Interpretation, User Manual”, from <http://www.malags.com>.